



Electroadhesion Cube Satellite

In Partial Fulfillment of the Requirements for NASA MINDS

Submitted by: California State University, Northridge
Matador Student Design



Advisor: Dr. Christoph Schaal

March 28, 2022

Team Members & Structure

Project Manager: Nareg Shirajian

MSD President: Nathan Gabriel

Mechanical Design

Lead: Matthew Awad
Brayan Gonzalez
Daniel Herrera
Nathan Gabriel
Eric Flores
Matthew Aralar
Jesus Sanchez
Christopher Rubio

Systems & Controls

Lead: Elliot Fayman
Arteen Galstyan
Martin Ha
Ruben Perez

Electroadhesion

Lead: Jiego Harel Judge
Nareg Shirajian

Testing & Simulation

Lead: Edgar Ovasapyan
Gerhardt Jurgens
Paula Logozzo
Justin Reust

Electroadhesion Cube Satellite

By: Nareg Shirajian, Elliot Fayman, Matthew Awad, Brayan Gonzalez,
Daniel Herrera, Nathan Gabriel, Eric Flores, Matthew Aralar, Jesus
Sanchez, Christopher Rubio, Arteen Galstyan, Martin Ha, Ruben Perez,
Jiego Harel Judge, Edgar Ovasapyan, Gerhardt Jurgens, Paula Logozzo,
and Justin Reust.

I have read and reviewed this paper prior to submission to NASA MINDS.

C. Schaal

Faculty Advisor Dr. Christoph
Schaal

03/28/2022

Date

Contents

1 Abstract	5
1.1 Motivation & Objective	5
2 Project Management	6
2.1 System Requirements	6
2.2 Subsystem Breakdown & Systems Engineering	6
2.3 Project Schedule	7
2.4 Project Cost & Budget	7
3 Mechanical Design	9
3.1 Design Overview	9
3.2 Finite Element Analysis	10
3.3 Conclusion	11
4 Electroadhesion	12
4.1 Theory & Research	12
4.2 Electroadhesion Design	13
4.3 Electroadhesion Testing	13
4.4 Conclusion	15
5 Systems & Controls	15
5.1 Systems & Controls Subteams	15
5.1.1 Radio	16
5.1.2 Attitude Determination and Control	18
5.1.3 Power	22
5.2 Conclusion	23
6 Testing & Simulation	23
6.1 Equipment & Testing	24
7 Conclusion	25
7.1 Current State and Future Plans	26
8 References	27

1 Abstract

The purpose of our project is to develop a swarm of cube satellites that will deploy bi-polar electroadhesive electrodes to collect and mitigate space debris. These debris, classified as "micro-meteoroids," can be categorized as large inactive satellites or a small speck of paint and are traveling thousands of miles per hour in Earth's orbit. Our objective is to develop technology using principles of electroadhesion and high voltage circuits that will be implemented to attract debris. The primary focus of collection will be on the small particles that are incredibly difficult to detect and track.

1.1 Motivation & Objective

The space industry has seen exponential growth in the last decade. The space race for satellites and human space exploration is more demanding than ever as private and government entities seek to expand and capitalize on their technologies. Both crewed and non-crewed payloads use rockets as the primary choice of transport to orbit. When a payload reaches its orbital speed, small or big particles are highly likely to get caught in Earth's orbit during stage separation. These particles can be part of a rocket booster, payload fairing, or even a speck of paint. These specific particles or debris are traveling thousands of miles per hour and have been classified as "micro-meteoroids." These particles pose a threat to expensive and sensitive space hardware and can even increase the risk in crewed missions. Moreover, different missions require different orbital trajectories, as satellites and crewed launches execute their missions for different orbital patterns and trajectories, so does the debris that is produced by them. An intersection of two different orbital trajectories can be catastrophic. Although these micro-meteoroids may seem to be insignificant in terms of size, their kinetic energy can be devastating. Matador Student Design is proposing a potential solution to help mitigate through collecting these micro-meteoroids by utilizing bi-polar electroadhesive electrodes to provide and ensure safer space travel, for both human and non-human explorations out in space. The team is planning to design and develop a cube satellite that will deploy the electroadhesive pad systems to capture micro-meteoroids in Low or Mid Earth orbit.

2 Project Management

2.1 System Requirements

During the system requirements review the conditions and requirements were determined and established. The goals of the project were intended to have purpose, qualities of being measured , and reasonably attainable. The physical characteristics of the cube sat was determined to be similar of a standard 1U satellite, which is about 4”x 4” x 4” cube that is equal to or less than 2.7 lbs. The satellite should be able to have a closed loop attitude control that is capable of minimum single axis control, for this specific requirement it was determined to use the reaction wheel method. The satellite should have capabilities of a radio communication system that is capable of transmitting and receiving data and sub-system status. The satellite should also be able to rely one hour solely on battery power and still be able to maintain full capabilities, in the event that the satellite is not in the field of view of the sun. In order for the satellites mission to be effective it must be able to deploy, power, and implement an electroadhesive mechanism such that it is able to attract or mitigate 1.5-oz of debris. Lastly, a custom micro-controller unit must be developed that is capable on controlling and processing all on-board sub-systems.

2.2 Subsystem Breakdown & Systems Engineering

In order to develop a satellite that is capable of space debris collection and mitigation, proper system engineering fundamentals must be implemented to achieve mission success. The project can be divided into a series project phases. Phase A: Concept and Technology Development, Phase B: Preliminary Design and Technology Completion, Phase C: Final Design and Fabrication, Phase E: Operations and Sustainability, Phase F: Closeout. Throughout these different project phases, consistent trade studies were conducted and constant feedback through design reviews were provided to ensure each team met their respective requirements.

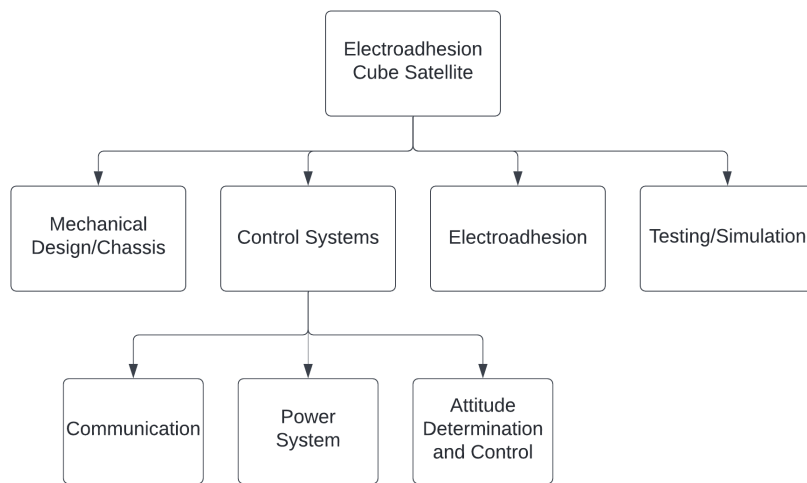


Figure 1: System hierarchy & Subsystem Breakdown

The team is comprised of four main teams: mechanical design, electroadhesion, control

systems, and testing and verification team. The purpose of the mechanical design team is to design and manufacture a satellite to the required specifications and ensure that all system components can be properly integrated. Control systems purpose is to provide the functionality of a radio communication system, attitude control and power distribution. Electroadhesion team is to research and develop the electroadhesion pads to collect debris in a safe and reliable manner. The testing and verification team is to verify the functionality of all subsystems through zero-g and vacuum environments.

2.3 Project Schedule

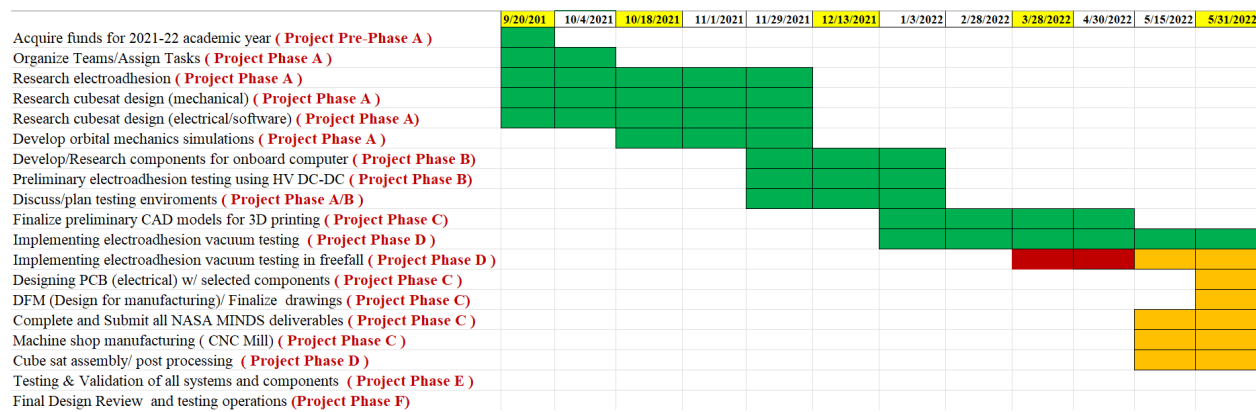


Figure 2: Project Schedule & Phases

The figure above is a detailed breakdown of the overall project schedule. As mentioned earlier the project can divided into different phases: Phase A: Concept and Technology Development, Phase B: Preliminary Design and Technology Completion, Phase C: Final Design and Fabrication, Phase E: Operations and Sustainability, Phase F: Closeout. Following the color coded scheme, the green indicates tasks and goals that have been met, the orange indicates future tasks and goals and the red indicates tasks that are overdue or have not been completed in its entirety. As indicated in the figure, the phases do not follow a consistent pattern and switch around depending on the subsystem, the reason for this issue is due to the fact that in the Fall, campus access and resources was still limited therefore hindering certain aspects of the projects. Notable dates that critical to the competition are, October 18,2021 is the due date to submit the proposal, December 15,2021 is the due date for the PDR document, March 28,2022 is the date when the systems engineering paper, project poster and the project video are due. If selected to continue, the team will then have to present the research to a live panel of NASA judges on April 30, 2022. Prior to the presentation, the team will also conduct a test readiness review to ensure all systems and procedures are operating at nominal conditions.

2.4 Project Cost & Budget

The budget hearing for the 2021-2022 academic year was announced in the early weeks of September and was determined to be \$3000 for the Matador Student Design team. These funds will be provided by our institutions “Associated Students” division, where it is responsible for the allocation and distribution of funds for student clubs and organizations.

It is worth noting that in the late months of spring 2021, Our team placed 3rd in the NASA MINDS competition and a result we were awarded \$1000. These funds were available in June and were consumed to further the research and development of last year project. A common component that is being reused from last year's project is the 'XP Power Q60-5 HV DC-DC Converter'. Additional funds may be available if our organization proceeds with fundraising, but due to COVID-19 regulations for the fall 2021 semester, access to campus and its facilities were limited and are currently still limited. Tabulated on the next page is the expected components and their respective costs. Adjustments have been made regarding price changes and extra material being required, therefore slightly increasing the cost for the cube sat development. Through experiment verification and validation it was concluded that bi-polar electroadhesive pads performed better than the uni-polar wire, resulting in additional costs to transition the design change. The calculated cost for one cube sat can start from \$2948.71. Note that certain components have been designated a certain color. The green refers to lab equipment that is used during research and development, the blue refers to general purpose items that are used throughout the entire timeline of the project, the orange refers to the components are that purchased in bulk therefore can be used multiple times, for example the 'Kapton Wire' comes in a spool with sufficient length that can be reused. Lastly, the yellow refers to the components that are needed and required per cube sat. Therefore, if a swarm of cube satellites were to be manufactured and assembled the cost per cube sat would be \$1749.81 after developing the initial cube sat since some of equipment and resources can be reused. The total cost for two cube satellites is expected to be \$4422.52. The expected cost for two cube satellites is within the \$4500 range that includes the funds from NASA MINDS and the funds that are provided by our institution. The \$1500 from NASA MINDS will be allocated to further our research and development of our cube sat and the electroadhesion technology, the additional funds will be used to expand more opportunities in the characterization of the electroadhesion by enabling us to potentially purchase more sensitive and precise equipment. Finally, it is worth noting that funds received by NASA MINDS will exclusively be used to for our project, and it will not be used to fund nor purchase anything that is not related to the success and progression of our project.

XP Power Q60-5 HV DC-DC Converter	\$344
AG60P-5 Surface mount HV DC-DC Converter	\$300
HV Probe	\$77.16
U3-HV LabJack DAQ	\$143.74
Kapton Wire KJL (16AWG)	\$67.50
FEA toolbar (Software)	\$77
Books/Technical Journals/Resources	\$100
Kapton Wire KJL (22AWG)	\$87.50
Polyimide Dielectric Film	\$100
Copper Foil/Shims	\$30
Arduino Nano RP2040	\$25.50
ATMEGA 2560	\$13.31
LSM6DSMTR (IMU) QTY. 4	\$17
Electronic Component Kit (Resistors, Capacitor, Transistors, etc.	\$20
3D Printer Filament/Accessories	\$100
Solar Cells (20-25% Efficiency)	\$60
OpenLST (Open-Source Radio)	\$50
Integrated Power Supply	\$40
Vacuum Chamber with Pump (3L)	\$100
Manufacturing (4 Walls) In house services.	\$100
Manufacturing (Outsourced components, Protolabs)	\$800
Unforeseen expenses (Price changes due to supply chains, Shipping costs, General Purpose tools and equipment)	\$300
Total Estimated Cost for QTY 1 CubeSat: \$2948.71	

Figure 3: Cost Analysis and Breakdown

3 Mechanical Design

The mechanical design team requirements are to develop a cube satellite that is identical in dimensions and weight of a standard 1U satellite. A 1U cube sat is a 3.94 in (10 cm) cube with a mass of approximately 2.2 lbs (1 to 1.33 kg). The goal is to design and manufacture the raw chassis that is capable of withstanding the loads that are presented during launch and safely contain all components of the picosatellite. During launch crewed mission can experience about 3.5g whereas non-crewed missions can be subjected to higher g during launch, around the range of 5-15g. Therefore the satellite is designed to withstand the loads under high acceleration. Lastly, The satellite should be capable of housing all its subsystems such as the communication system, power systems, altitude control system and the electroadhesion system. Solidworks 2021 is used to model our design as well as run analysis using finite elements.

3.1 Design Overview

In the early design process the considered materials were 6061-T6 aluminum alloy and 7075-T6 aluminum alloy, it was later concluded that 7075 alloy would be the better candidate due to its thermal and material properties. 7075-T6 Aluminum, the chosen material, has a tensile strength that is 1.76 times that of 6061-T6 Al, shear strength that is nearly 1.5 times that of 6061-T6, as well as being substantially harder. 7075-T6 aluminum is slightly more corrosive resistant than 6061-T6 Al. These properties can be seen in Table 1 below.

Table 1 Material Properties

Properties	6061-T6 Al	7075-T6 Al
Yield Strength	40 ksi	73 ksi
Ultimate Tensile Strength	42 ksi	74 ksi
Modulus of Elasticity	10000 ksi	10400 ksi
Poisson's Ratio	0.33	0.33
Thermal Conductivity	1160 BTU - in/ hr-ft ² -°F	900 BTU - in/ hr-ft ² -°F
Melting Point	1080-1205°F	890-1175°F
Density	0.0975 lb/in ³	0.102 lb/in ³
Machinability	Good	Fair

The best design for the chassis was determined to be a 4"x4"x4" cube with simple geometry of an X-like pattern and large slots on the faces of the cube to maintain strength and minimize weight. We went through 4 different designs for the chassis. Through design reviews and simulations, we have changed geometry, components, ideas, and materials which brings us to the current design of chassis V4. This design meets the design size requirements of weight at 0.69 lbs, dimensions, and minimum FOS at 2.136. The design meets our requirements of weight, size, and compatibility and is also optimized for machining. Designing for machining means that each part is made to the availability of tools and tool geometry of the equipment used for manufacturing. The size of the machining tool limits the machinability of a part. The internal features of a part can not have 90° geometry because the radius of the tool cannot make that turn without risk of breaking the tool

and the part. External features are not as limited to tool geometry because the tool is not engulfed by material, it has more freedom around the part. These machining limits can be solved by creating fillets on internal features to allow for the tool to do its work with less resistance and a smoother cut. Creating holes and geometry in standard sizes is great practice due to the availability of standard size tools and the amount of time saved by using standard size tools. For our design overview prototype, we 3D printed the chassis and its components using polyimide (PLA) plastic material. Moving forward we will be 6061-T6 Aluminum for the structural prototype, and 7075-T6 Aluminum for our launch ready satellite. When researching manufacturing of this model, we are looking at metal 3D printing and CNC machining. With CNC machining, we would be able to get the machined parts completed on-campus in our machine shop but we have to supply the material. With outsourcing and metal 3D printing, our cost would be much higher but can be done in a quicker manner. As of this paper, we are going to CNC machine the parts and assemble the chassis.

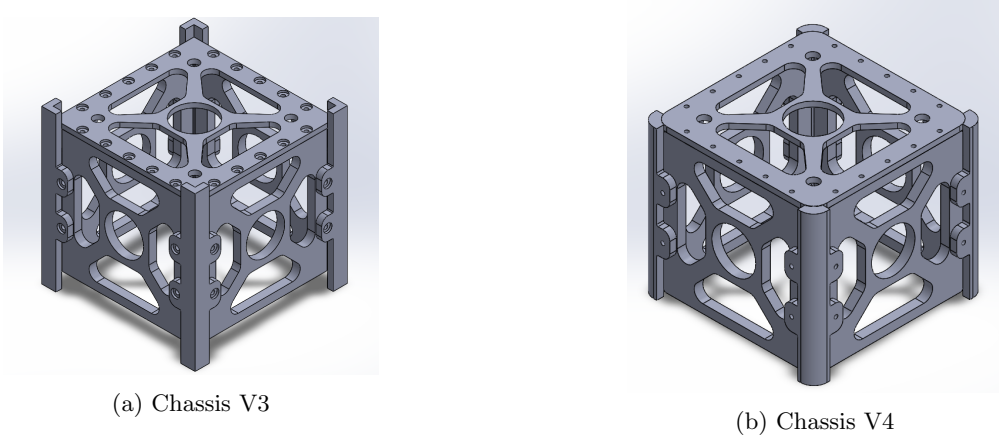


Figure 4: Chassis V3 and V4 are

3.2 Finite Element Analysis

Finite element analysis was conducted to verify the structural and the thermal properties of the design. A variety of studies were conducted such as stress analysis, frequency analysis, and the stresses caused by thermal loads. During the launching process is when the satellite would experience the maximum and critical loads. To simplify the studies and avoid the risk of a non-convergent study, the studies were conducted on the raw chassis. A mass of 0.69 lbs was calculated and a force of 25N was applied on the entire chassis. According to NASA technical standards for metallic structures the allowed factor of safety (FOS) for non-crewed flights is between 1.25-1.4. Results showed that we were able to obtain a FOS of 2.14 during launch conditions and a FOS of 1.60 for the thermal stress study. The studies are ran with a high quality mesh and global element size of 0.1 inches which reaches mesh convergence.

The significant thermal stresses would be present when the satellite is on its orbital path, where temperatures can be as low as -274°F and as high as 266°F. Insulated spacecraft

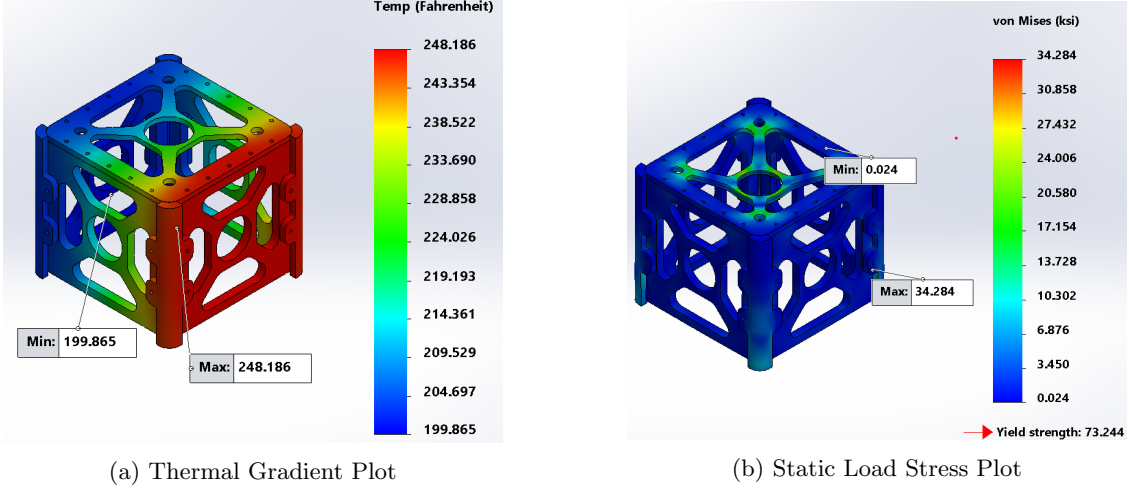


Figure 5: Resultant plots of static load study and temperature study

and satellites would have a smaller range. The boundary conditions for the steady state radiation study were 248°F thermal load, -40°F ambient, and emissivity of anodized aluminum is 0.77. The static load with the forces of launch yields results of a max Von Mises Stress of 34.284 ksi and a yield strength of 73.244 ksi.

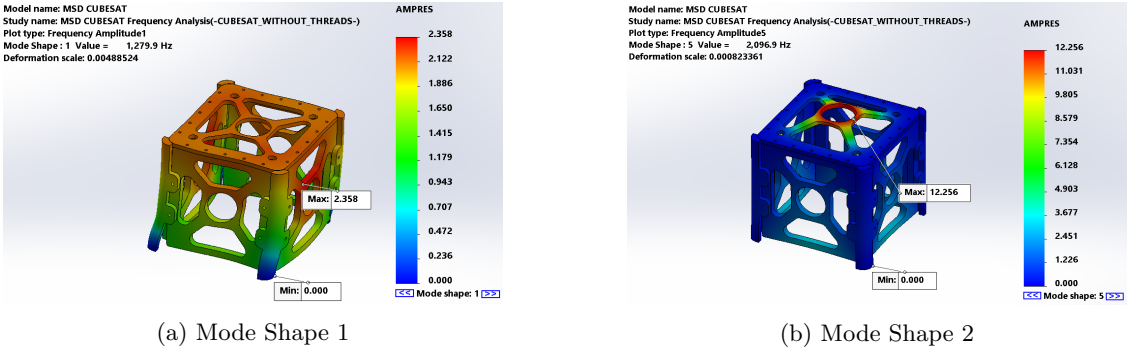


Figure 6: Comparison of the lowest and highest resonant frequency

Results showed that in a steady state scenario there will be a 48.33°F difference between the exposed side and non-exposed side. The final study that was conducted was a modal analysis during the launching conditions. The boundary condition is a fixed constraint on the bottom of the 4 support columns. The results showed the lowest resonant frequency of the structure to be 1,294 Hz and the highest to be 2,115.6 Hz.

3.3 Conclusion

Within the context of this work, the structural frame of our cube sat is designed and analyzed using finite element method via Solidworks 2021. After the design reviews, we have further optimized the structural chassis in weight and geometry. The raw chassis is weighed at 0.69 lbs which meets our design criteria. Results showed that we were able to obtain a FOS of 2.14 during launch conditions and a FOS of 1.60 for the thermal stress study. Our chassis meets the requirements of weight, dimensions, capability of storage, and Factor of

Safety. This chassis can handle the 18 g's (yield) of acceleration during launch. The structural chassis design will transition to manufacturing when we receive our parts and materials in the upcoming weeks. Moving forward, we will be adding all components of the picosatellite into the chassis with the solar panels physically and in the CAD. In conclusion, our chassis is a decent model and meets the requirements.

4 Electroadhesion

Electroadhesion (EA) is the electrostatic attraction between two objects when an electrical potential is present. A popular implementation of this effect can be characterized by developing EA pads which are composed of an electrode and a material whose dielectric constant is relatively large, the electrode will then be placed between two pieces of the dielectric material and then subjected to high voltages ranging from 2 to 8 kV. A common approach of the development of an EA pad is to use co-planar bi-polar interdigitated electrodes using copper or aluminum, where one electrode is energized and the other is not energized which results in an electric potential and creates electrostatic charges on the surface of the dielectric material. The dielectric material that is commonly used for this application is polyimide.

4.1 Theory & Research

Substrate concentrations would be concerning micro-meteoroids and space debris, which vary from small paint chips, fragments of launch vehicles, and pieces of composite or space dust. The method of capturing these small, undetectable micro-meteoroids and space debris is through electroadhesive pads. The electroadhesive pad is energized by using a high voltage DC through an HV DC-DC Converter from a low voltage power supply. This allows static charges to accumulate on the EA pad, polarizing the object of focus, such as a small aluminum chip from a rocket. In Figure 8 below, a schematic that shows the electric field created between energized electrode and the neutral electrode as well as the geometry of the selected pad is shown.

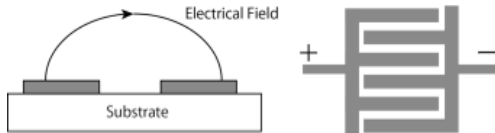


Figure 7: Electroadhesion Pad Schematic

$$F = \frac{A * \epsilon_r V^2}{2 * d^2}$$

The equation above is a general formula for determining the force for a electrostatic pad. where A = contact area, ϵ_r = dielectric constant, V = applied voltage, and d = dielectric thickness.

The figure above portrays an electrostatic simulation that was developed on MATLAB. The simulation shows a small section of the electric potential distribution of an interdigitated electroadhesive pad. The white, rectangular templates represent the copper electrodes.

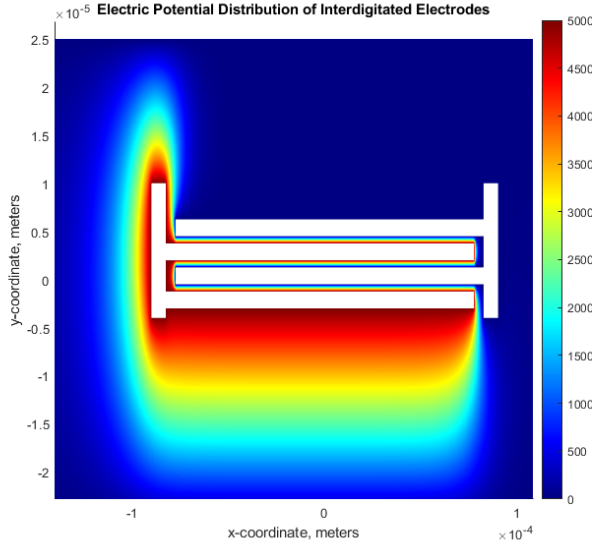


Figure 8: Electroadhesion Pad Simulation

4.2 Electroadhesion Design

The objective of the electroadhesive pad design is to be able to utilize electrostatic force to attract substrates through charged particles. This is through the use of a High Voltage (HV) DC-to-DC converter to produce approximately 5 to 6 kV output using a 5 volt input from an external power supply, a microprocessor, or a function generator. For the designs below, these allow oppositely charged particles on each side. Electroadhesive pad assembly samples were manufactured by hand with two different thicknesses of copper film and Kapton polyimide films. It also has variations in length-to-width teeth ratio of the interdigitated pattern.

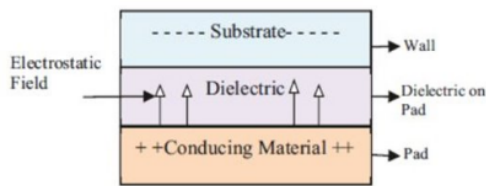


Figure 9: Electroadhesion Pad Diagram

4.3 Electroadhesion Testing

The difficult part of working with electroadhesive pads were design choices, as testing of various samples were done with the same Aluminum filings, as well as larger test controls such as concrete, wood, and plastic. All samples except for the wire and wire-coil combinations exhibited adherence to the concrete, wood, and plastic substrate. Trial with aluminum and steel filings displayed a less anticipated reaction even at 6 kV output from the step-up converter. Latest sample pad was manufactured using an existing 3D printed tem-

plate for copper electrodes, an adhesive-sided Kapton polyimide film, and a non-adhesive polyimide film of the same thickness. Testing involved isolation in a vacuum chamber and with air. The latest EA pad revealed activity of adhesion with a small amount of aluminum chips. Further designing of how to adjust the length-to-width teeth ratio may improve the adhesion activity, as well as precise manufacturing of sample pads for testing improvements.

It is difficult to assess how different and significant the differences in terms of electric potential, electrostatic force (attraction force), and the length-to-width teeth ratio. As seen on Fig. 10, the most up-to-date planned manufacturing for a set of copper electrodes will be done using a wire EDM (electrical discharge machining) method that is available in our university. Afterwards, as soon as sample pad iteration is manufactured, another set of testing with debris will be done regularly on ground and inside an insulated vacuum chamber.

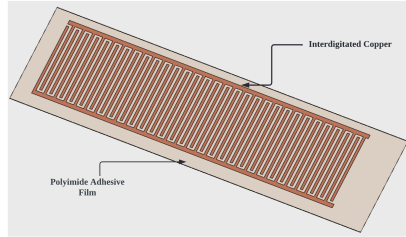


Figure 10: Electroadhesion Pad CAD

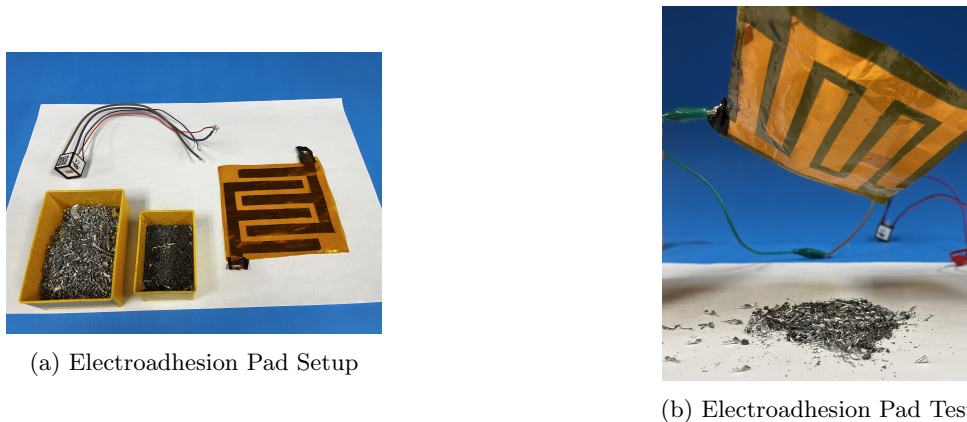


Figure 11: Electroadhesion Pad Setup and Test

Fig. 11 exhibits the set up and goal of the electroadhesive pad where the main components of the system are the HV DC-DC converter, a few steel and aluminum "dusts" to represent space debris, and the handmade electroadhesive pad. Upon contact of the EA pad against the debris, testing showed that it was possible to utilize this type of technology to capture the represented space dust. It was also suggested that by shrinking the length-to-width teeth ratio of the electrodes, it could possibly be strengthen the grip of the electrostatic force. During the testing process in Figure 11 b) it was observed and recorded that when particulates and debris adhered to the EA pad the current readings from the

power supplied dropped and when the debris was removed the current readings increased, this observation was tested multiple times and it deemed to be repeatable, therefore it has been concluded temporarily to be a measurement metric for the amount of debris adhered to the pad.

4.4 Conclusion

Research suggests that the most efficient design to be used when constructing electroadhesive pads were the interdigitated pattern, it is still a possibility to utilize a unipolar approach when it comes to providing a more controlled way of avoiding attraction between multiple electroadhesive pad systems. The final state of the electroadhesive design will be manufactured in a professional setting to increase the efficiency of the current design, as well as to make sure that jumping voltage or voltage breakdown occurs during the process of attracting space debris or testing phase.

5 Systems & Controls

5.1 Systems & Controls Subteams

The System & Controls design team was in charge of creating a command and data handling (C&DH) infrastructure within the cube sat that would allow it to maintain a start-up sequence daily, control power, and act as a hub so that the various components of the cube sat could communicate with each other.

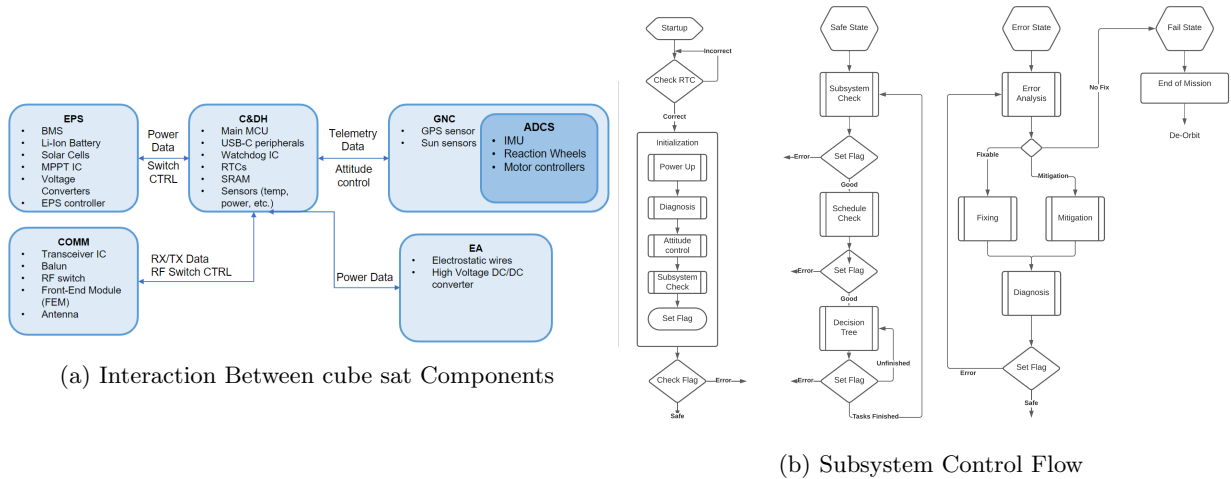


Figure 12: Current System & Controls Design

To add to this, The current C&DH system consists of the microcontroller unit (MCU), USB-C peripherals, Watchdog IC, real-time clocks (RTCs), static random access memory (SRAM), and sensors (temperature, power, etc.). The MCU is the primary component of the C&DH system as it would be the component to store and run programs. Consequently, the team settled for an MCU with requirements based off the Arduino Mega (ATMega2560) features, most notably for its clock speed of 16MHz, a flash memory of 256kB, and 8kB of Ram. As a result, a C&DH schematic was created using EasyEDA, a web-based EDA tool allowing the design of schematics and printed circuit boards.

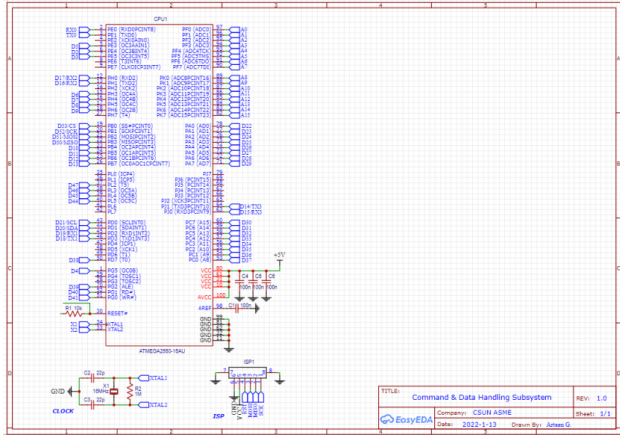


Figure 13: Control Schematic using EasyEDA

Once the schematic was finished, a prototype was developed using a breadboard, an ATMega2560 MCU soldered on a breakout board, and an Arduino Uno to upload code to the MCU.

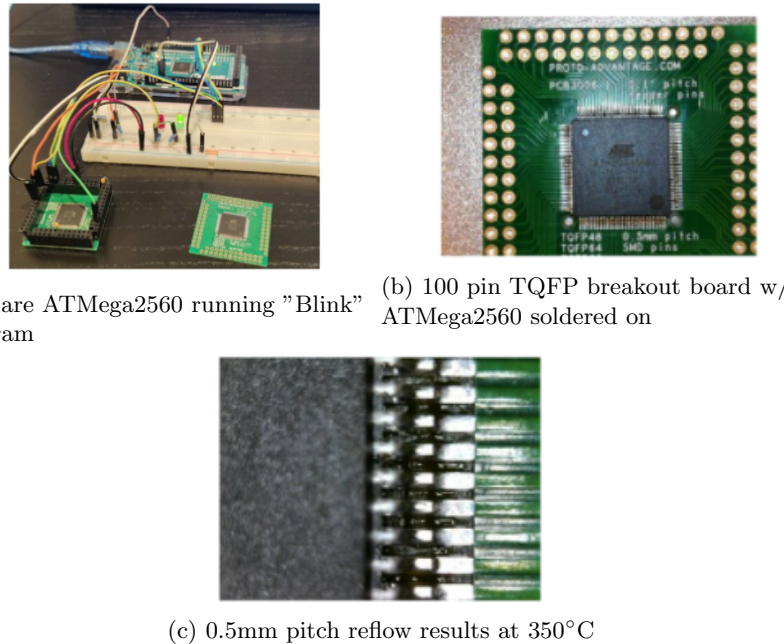


Figure 14: Command and Data Handling Prototype

5.1.1 Radio

The radio design is based off of OpenLST, an open-source radio design that utilizes cheap commercial components for communications with distant instruments. OpenLST is a proven radio design as its parts are based off of a public Earth imaging company, Planet, whose Dove LST (Low-Speed Transceiver) radio has had an extensive history of successes and reliability.

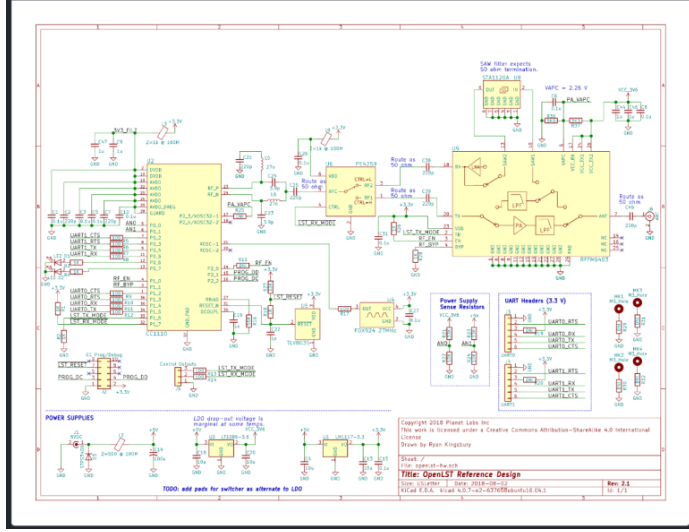


Figure 15: OpenLST Radio Design

In order to create the radio, EasyEDA was used to design the radio’s circuit schematics, footprints, and PCB layouts. The team opted for a simple RF circuit design following four important developmental rules: the use of 4 layers, integrated chips (IC), a standard of 50 ohms everywhere, and routing the radio frequency (RF) first.

The idea of the four layer PCB board allows for an easy design while allowing any part of the board to connect to the ground plane with easy access by simply dropping a via almost anywhere. The use of integrated chips comes with the benefit of being small, cheap, and reduces the amount of work needed. The standard of 50 ohms everywhere (output, transmission, input), reduces the need for impedance matching, which would otherwise create the need for tedious calculations using a Smith chart, significantly saving time and reducing unneeded workload. Furthermore, the choice of 50 ohms is based of the notion that it is an industry-standard and many manufactured components tend to target the 50 ohms interface. Lastly, the reason for routing the RF first is prevent other signals away from the RF. Furthermore, when routing the RF, traces were kept short and direct, relative to wave length as the effects of wavelength become more prominent the higher the frequency or the larger the design. To determine wavelength, the following formula can be used:

$$wavelength = \frac{lightspeed}{frequency}$$

For its implementation, the radio will have receive data about the cube sat’s state, either safe state or error state, from the Control and Data handling system via UART communication once a day.

The C&DH system will signify the radio that it has data to transmit and switches the cube sat to high power mode. From there, it will transmit the data back to ground within a 432-438MHz. Accordingly, our team can then transmit a solution back to the cube sat and attempt to resolve the issue, whatever it may be. The radio then checks for any up-link data or commands from ground and sends it back to the C&DH system. Once the issue is resolved or no additional commands have been given, the C&DH system will switch the cube sat back to low power and the radio will not transmit or receive data, signaling the

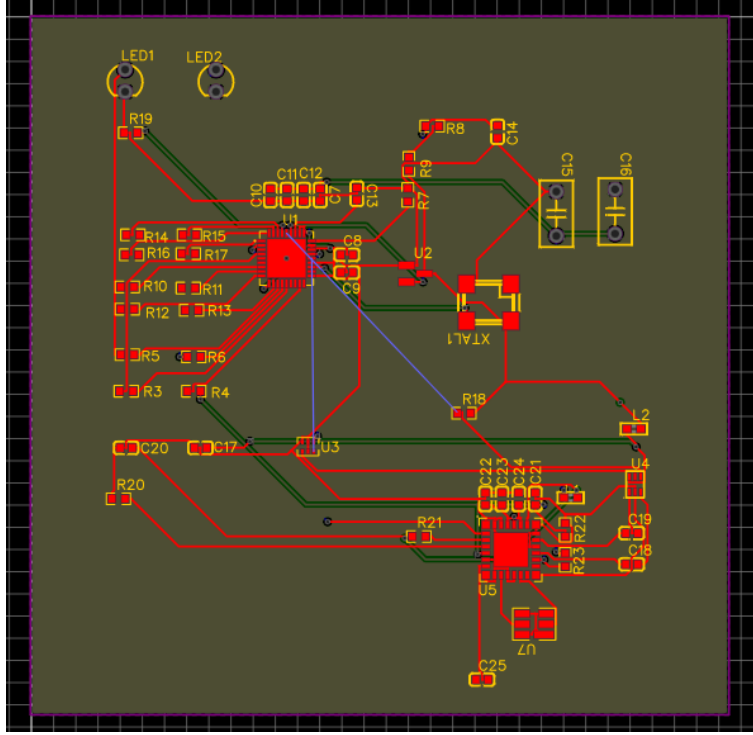


Figure 16: Current PCB Design

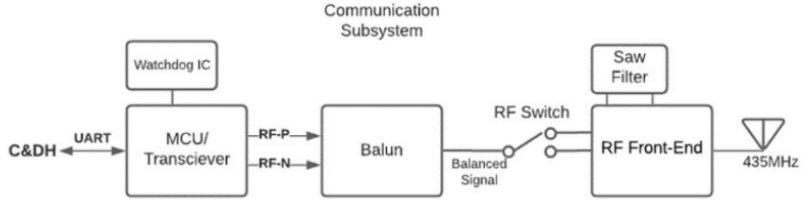


Figure 17: UART communication w/ C&DH System

completion of its daily routine.

5.1.2 Attitude Determination and Control

Upon deployment, the cube satellite is expected to rotate due to an external torque from the cube satellite deployment system. The exact speed of the rotation is entirely dependent on the specific launch mechanism however, most cube satellite literature agree on a rotational speed of 1 radian per second or lower. This is problematic because the cube satellite is entirely dependent on its solar panels for power and by not maintaining a constant attitude that maximizes power generation, the cube satellite will be at risk of running out of power. In order to ensure a particular, constant attitude, two steps must be taken: 1) determine the current angular velocity 2) correct the angular velocity. To determine the angular velocity, an MPU-6050 (3-axis gyroscope) will be used due to its low cost and good documentation. To correct the angular velocity, also called detumbling, a magnetorquer, reaction wheel, or thruster could be used. After some preliminary research, a reaction wheel

was chosen due to its lower cost of development as well as its popular use in attitude control subsystems for other cube satellites.

Inertial Measurement Unit

The MPU-6050 is a micro electro-mechanical system with a three-axis accelerometer and a three-axis gyroscope. The gyroscope and accelerometer can communicate with an Arduino microcontroller via the I2C protocol. After plotting the data from the three-axis gyroscope, it was discovered that the MPU-6050 tended to generate some high frequency noise. This is problematic because if this data is sent directly to the reaction wheel, it might make sporadic movements in direct response to the sporadic data being sent that could damage components of the cube satellite or even lead to a unrecoverable tumble.

To attenuate the high frequency, a low pass filter must be implemented. Ideally, the low pass filter will create a "Brick wall" perfectly eliminating all signal past a certain cutoff frequency. However, no such filter exists without an additional side effect. Ideally, the filter that would be implemented would closely preserve the signal before the cutoff frequency while performing significant attenuation on any signal past the cutoff frequency. Four different type of low pass filters where considered: Bessel, Butterworth, Chebyshev, and elliptic.

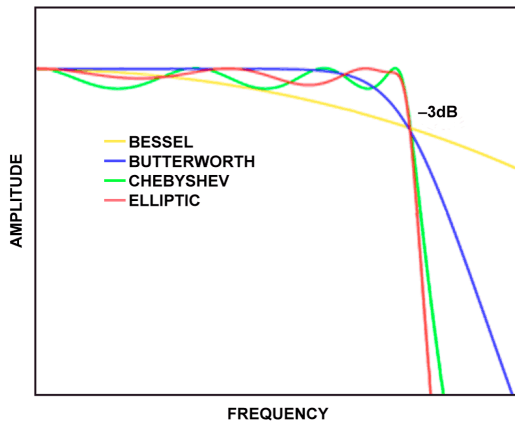


Figure 18: Effects of Filters

The Chebyshev and elliptic filters both attenuate the signal past the cutoff frequency very well but add extra noise to the signal before the cutoff frequency. The Butterworth filter does not add extra noise before the cutoff frequency however, it does not perform the attenuation of frequencies past cutoff as well as chebyshev and elliptic. The Bessel filter performs the worst adding noise to signal before the cutoff while not attenuating signal past the cutoff not nearly as well as the Butterworth, Chebyshev, and elliptic filters. Because the most important attribute of the filter is its ability to preserve frequencies before the cutoff frequency, the Butterworth filter was chosen. The last parameter that must be determined before the filter can be fully implemented is the order of the filter. The higher the order, the closer the filter will mimic a perfect brick wall filter however, as a side effect, their will be increasingly larger phase shifts in the filtered data. This will have the effect of creating "delays" in the data as it is being processed, so it would be best to minimize the phase shift. A 2nd order Butterworth filter attenuates the frequencies past the cutoff adequately while minimizing the phase shift.

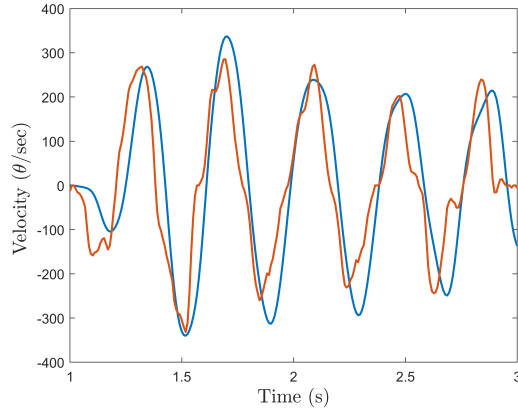


Figure 19: Phase Shift with 2nd Order Butterworth filter

Reaction Wheel The reaction wheel is composed of two components: the motor and the inertia wheel. The characteristics of the inertia wheel are entirely dependent on the characteristics of the motor. Since the 3V DC topox motor that was selected has a low torque and spins at 1730 rotations per minute, the inertia of the wheel must be relatively small. To spin a satellite using a reaction wheel, you can either spin a heavy wheel slowly, or spin a light wheel fast. The inertia wheel that will be used is a small 3d printed disk with washers glued on top to add additional weight. To determine the maximum speed the reaction wheel can spin the satellite, we can use the conservation of angular momentum since the satellite experiences relatively little external forces while it is in orbit:

$$L = I * w$$

$$L = I_{sat} * w_{sat} \quad \& \quad L = I_w * w_w$$

$$I_{sat} * w_{sat} = I_w * w_w$$

$$w_{sat} = \frac{I_w * w_w}{I_{sat}}$$

$$w_{sat} = \frac{1730 * 0.0012}{0.194}$$

$$w_{sat} = 11.379 \text{ rad/s}$$

If the reaction wheel from rest spins up to its maximum speed, the satellite can obtain an angular velocity of 11 rad/s. The maximum tumble rate is 1 rad/s so, after detumbling, the reaction wheel will have plenty of available angular momentum to impart on the satellite to correct for long term negligible forces like solar wind or tidal forces before the motor becomes over saturated.

Proportional Integral Derivative Controller

In order to detumble the satellite, the motor must be told to maintain various, constantly changing speeds. For this reason a closed loop controller is needed in order to accurately

control the motor speed. this can be achieved with a Proportional-Integral-Derivative (PID) controller. A PID controller continuously calculates an error value which is the difference between the desired angular speed called the set point and the measured angular speed called the process variable. The error is then processed based on a proportion of the desired angular speed and the actual angular speed (Proportion), the constant error of the angular speed (Integral), and the predicted future values of the angular speed (Derivative). The weight of each part of the controller P, I and D can be changed in order to optimize the accuracy and speed at which the desired angular velocity is reached which was completed during testing. For this satellite, the process variable is calculated using the filtered data from the MPU-6050 which is then sent to an Arduino Uno microcontroller to be processed and finally sent to a BD65496MUV, a DC motor driver, that gives the correct voltages to the DC motor.

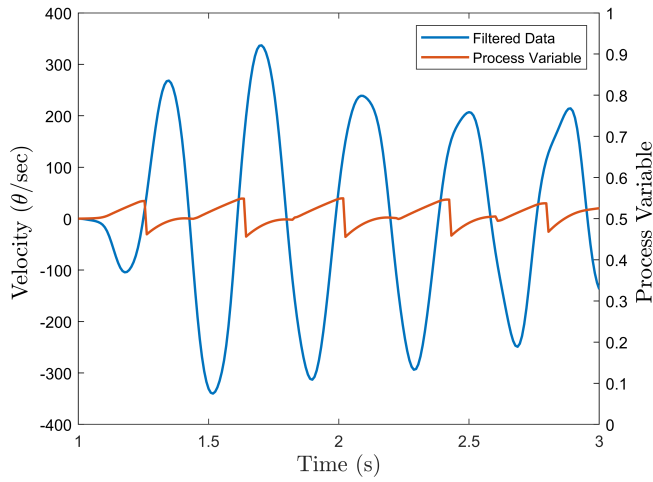


Figure 20: Process Variable vs Time

Prototype In order to verify the effectiveness of the reaction wheel and tune the weights of the PID controller, a physical prototype of the entire assembly must be made. To create the chassis of the satellite, a 3d printed PLA copy was created. In the final version of the satellite, the electrical components would be stored in shelves inside the satellite. However, the 3d printed chassis is less than half of the weight of the real chassis so the moment of Inertia will be dramatically different if the placement of the electronics is mimicked. For this reason, the electronics were mounted on the outer surface of the 3d printed chassis in order to increase the moment of inertia to closer represent the moment of inertia of the final satellite. To properly test the reaction wheel, the satellite must be able to be spun in one axis with minimal friction. This was achieved by placing the prototype on a thrust bearing and then mounting that thrust bearing inside a bearing block. This way, the reaction wheel, that is mounted on the bottom plate, can be used to test its effectiveness in a single axis. To optimize the weights of the PID controller, each weight was tuned separately by increasing or decreasing it and then seeing its effect on the cube satellite after programming the reaction wheel to resist any additional rotational motion.

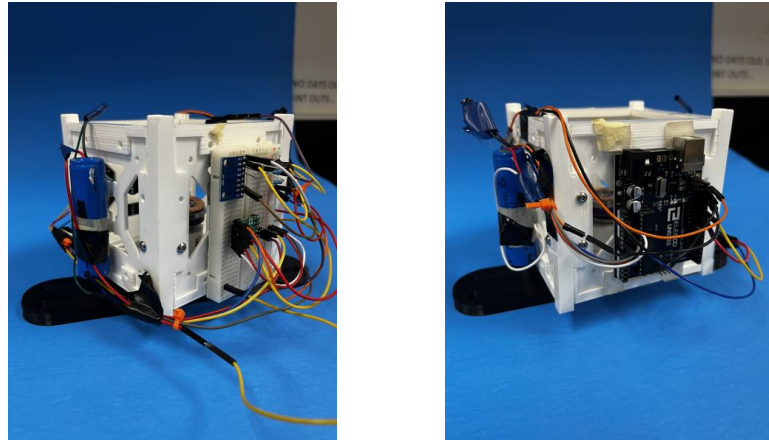


Figure 21: Breadboard prototype of Reaction Wheel

5.1.3 Power

The power subsystem is in charge of maintaining maximum power efficiency for the cube sat. The power budget is expected to be 50Wh a day, not including the power consumption of the power subsystem. The 50Wh estimate is derived from the constant power consumption from the Controls and Electroadhesion systems, roughly 1.8W or 43.2Wh a day, added with the radio power consumption, 4.4Wh a day, for which the radio will be transmitting and receiving data for roughly 30 minutes each. With that being said, the current design plan is to have a power subsystem consisting of a power management integrated circuit (PMIC), a batteries, and solar cells. The PMIC must be able to output 5V (high-power mode) and 3.3V (low-power mode). Additionally, it is required that the PMIC must also be able to deliver roughly 1.6A to the radio while it is transmitting. Moreover, the batteries of the cube sat are comprised of two parts, the primary batteries and the secondary batteries. The primary batteries are non-rechargeable and are used for a one-time short use, usually during or after the cube satellite's launch. The secondary batteries are rechargeable batteries that are replenished using the solar cells found on the cube sat. These secondary batteries are the main source of power for the cube sat during its lengthy mission. The solar cells are expected to have a wattage greater than 4.2W, assuming that the cube sat is in sunlight for at most 12 hours per day.

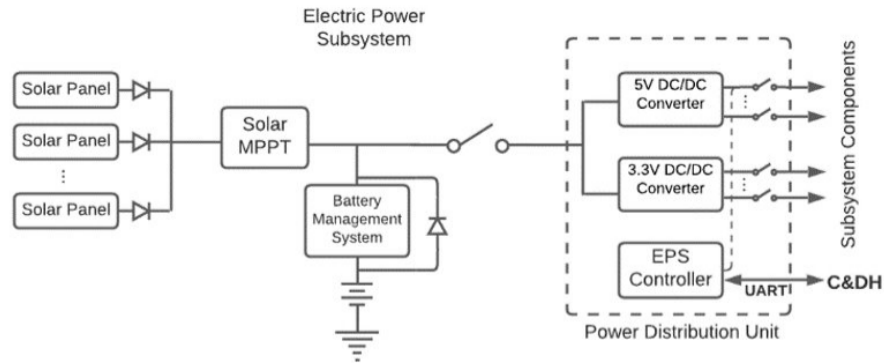


Figure 22: Electrical Power Subsystem

On top of that, load switches, an electronic component that connects loads to a power supply, will be controlled using a microprocessor in order to power up, down, or even save energy when certain loads are not needed. To add to this, maximum power point tracking will be used for the solar array in order to optimize power consumption.

5.2 Conclusion

When the satellite is deployed, the satellite will use a reaction wheel to detumble and adjust its attitude such that it will remain directed towards the sun. That way, the solar panels on the satellite will produce maximum power to support all critical and auxiliary electronics such as the electroadhesion device and the OpenLSt radio.

6 Testing & Simulation

The objectives of the Testing and Simulation sub-team is to verify the functionality of all the subsystems by simulating a zero gravity vacuum environment, and generate astrodynamical simulations using FreeFlyer. Utilizing FreeFlyer, the testing sub-team is responsible for orbital simulations that include potential flight paths, altitude data, orbit time, total sunlight time per orbit, and the angle between the sun and the solar panel array to determine the most optimal orbit path. The team was able to plot a two-dimensional and three-dimensional map of the orbit path that our cub sat is expected to take throughout its entire simulated orbit.

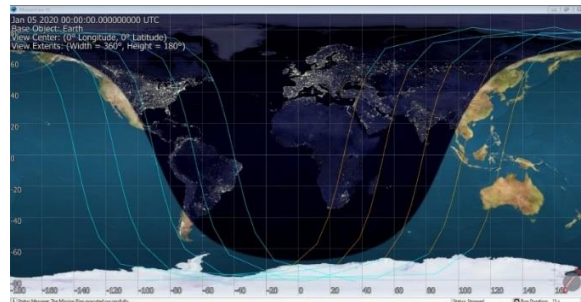


Figure 23: FreeFlyer Main Orbit Simulation 2D Map

In Figure 23, a screenshot of a simple 2D map that FreeFlyer outputs for the cube satellite's selected orbit path. We can output data such as longitudes, latitudes, numbers, and epochs to assist with the determination of which orbit path to take. If we find that an orbit path is not valid for whatever reason, we can edit the simulation to output data on a different orbit path that will be free of unwanted obstacles. We may also edit the simulation to place our cube sat in a denser debris field to maximize effectiveness. With the integrated GUI and free-form scripting language, we can efficiently output data that will provide us with the necessary information to avoid radiation damage. Specifically, avoiding things like the Van Allen belt is crucial to preserving and protecting the components of our cube sat. Our systems team will also utilize the distance from the cube sat to the Sun during its orbit to optimize the solar panels.

CubeSat.Date/Time	SunPanelAngle (°)	CubeSat.Range.sun (km)
Jan 01 2020 00:00:00	0.000	147103803.159
Jan 01 2020 00:05:00	0.000	147102319.004
Jan 01 2020 00:10:00	57.729	147100457.294
Jan 01 2020 00:15:00	74.162	147098403.179
Jan 01 2020 00:20:00	90.877	147096360.374
Jan 01 2020 00:25:00	107.577	147094531.097
Jan 01 2020 00:30:00	123.957	147093096.495
Jan 01 2020 00:35:00	139.415	147092199.019
Jan 01 2020 00:40:00	152.188	147091928.080
Jan 01 2020 00:45:00	157.089	147092310.503
Jan 01 2020 00:50:00	149.948	147093307.204
Jan 01 2020 00:55:00	136.332	147094816.924
Jan 01 2020 01:00:00	120.578	147096686.778
Jan 01 2020 01:05:00	104.072	147098728.171
Jan 01 2020 01:10:00	87.321	147100735.998
Jan 01 2020 01:15:00	87.321	147102508.948
Jan 01 2020 01:20:00	87.321	147103869.089
Jan 01 2020 01:25:00	87.321	147104679.263
Jan 01 2020 01:30:00	87.321	147104856.877

Figure 24: FreeFlyer Main Orbit Simulation Angle Data

In Figure 24, a screenshot of the angle with the sun data that we are able to get FreeFlyer to output.

6.1 Equipment & Testing

Along with being responsible for the orbit simulations and data, the testing and simulation team is verifying the effectiveness of the electroadhesion prototype using a vacuum chamber and a drop rig.

A vacuum chamber with the electroadhesion wires suspended inside, will be dropped from a sufficient height to simulate a zero-gravity environment. In addition, debris particles will be included in the chamber to simulate debris the cube sat will encounter while deployed. These tests will yield valuable data to evaluate the effectiveness of the debris collection. The vacuum chamber being used in testing is a standard aluminum chamber with a rubberized gasket lid and pressure inlet/outlet valve. The chamber has a height of approximately 9.50 inches without the lid, and a height of approximately 10.75 inches with the lid. The diameter of the pot, not including the handles, is approximately 10.90 inches. This chamber will house the electroadhesion apparatus inside, with the debris samples and other data acquisition components on top during free-fall tests. The overall chamber weight is predicted to be no greater than 10 lbs., which is an important figure to determine for free-fall testing. In order to verify the functionality of the electroadhesion prototype, the prototype must be tested in an environment that is as close as possible to the environment that the satellite is expected to operate in - namely, the micro-gravity environment of a low-earth orbit satellite path. To simulate micro-gravity, the testing team determined that the electroadhesion apparatus should be subjected to free-fall. This is achievable through the usage of a drop rig, which is a safety device that allows the electroadhesion apparatus to fall for several seconds before arresting the motion of the apparatus to prevent impact with the ground. The chamber originally had no electrical port through which a current could be routed to power the electroadhesion apparatus. To solve

this problem, a 1-inch diameter hole was drilled through the plexiglass. A corresponding 1-inch diameter socket was designed in SolidWorks and 3D printed, then fitted into the hole. The socket was sealed in place using a two-part epoxy to prevent gas from leaking through the socket fitting. The socket was threaded with copper wiring, then sealed again with the same two part epoxy. To test the integrity of the vacuum, the chamber was evacuated to -0.9 ATM (based off of the pressure gauge) with the new socket in place, and left untouched over the weekend to determine whether any leakage occurred. It was found that the pressure gauge remained at -0.9 ATM, verifying that the socket was airtight.

Methodology: To simulate the space debris that the apparatus would be collecting in space, a controlled amount of metallic shavings were placed inside the vacuum chamber. The critical information being collected from these trial runs includes speed of adhesion, magnitude of attraction between electroadhesion wires and debris, and total fraction of sample material adhered during each trial. To assist in gathering this data, a small camera will be mounted to the lid of the vacuum chamber to provide real time visual information for each individual trial run. After each test, the fraction of unadhered material will be weighed to determine the percentage of the sample that adhered to the wires. This will help to ascertain the effectiveness of the electroadhesion wires for a wide range of debris material types and will inform future iterations of the electroadhesion design process to improve adhesion efficacy. Freefall tests will be conducted from the rooftop of a five-story building to have enough time in freefall for the debris to adhere to the wires. It is predicted that the drop distance will provide roughly 1.6 seconds of freefall time, which was determined to be sufficient for adhesion purposes. The vacuum chamber itself will be attached to a high-tension cord and spring system to prevent impact with the ground.

Drop Rig: The drop rig is constructed of 1.25" 1045 steel box tubing. The box tubing stock was first cut with a saw, then welded into its final shape. The rig is designed to clamp around the rooftop retaining wall of the CSUN campus parking structure. It is also designed to suspend the vacuum chamber approximately 1.5 feet away from the wall of the parking structure to prevent any collision between the vacuum chamber and the wall during freefall. Collisions during freefall will impact the validity of the experiment and should be avoided. When deciding on the rope and materials used to drop the vacuum chamber, the maximum force on the chamber can be found with $F = mg(mg)2 + 2kmgh$, where k is the combined spring constant of the rope and spring attached to the vacuum chamber. Figure 25 is a graph of the falling force with respect to the spring constant to determine the maximum force on the vacuum chamber with a selected cord and spring.

7 Conclusion

As industries seek new frontiers in space and human exploration, the byproduct of debris generation becomes inevitable. Matador Student Design proposes their research as a potential solution for this growing issue in our orbit. To maintain a sustained human presence on the moon and mars, space travel and exploration must be a low risk endeavor. Through the application of system engineering fundamentals, the development of this research can continue to expand and improve.

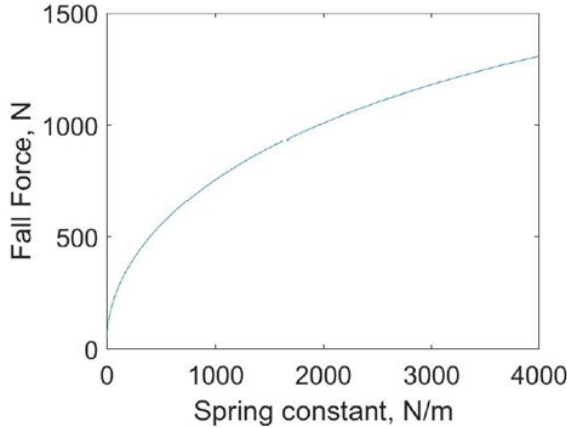


Figure 25: Fall Force vs. Spring Constant of Simulated Free Fall

7.1 Current State and Future Plans

As of now, the project is transitioning from research and develop to fabrication and verification. the FEA analysis for the cube satellite chassis has been completed and the mechanical design subsystem team is pivoting to optimizing the current design for inexpensive manufacturing. the electroadhesion subsystem continues to make additional prototypes of the EA pads including testing various geometries. A vacuum sealed drop test of the EA pad design is planned in order to verify the electroadhesive properties in a zero g vacuum. Systems and Controls suffered a set back due to the added lead times and increased cost of electrical components due to impacted supply chains. Despite this, the systems controls team is gradually obtaining and testing each component as it arrives. In the short term, a fully functional prototype with every subsystem being integrated will be produced in less than a month. In the future, the plan is to further reinforce the satellite for the hostile environment of space including making electronics and software radiation hardened. Further testing of the EA subsystem is also planned with the goal of producing a more refined and optimized design. Lastly, the goal would be to send many of these satellite to space so development of satellite to satellite communication and interaction is planned.

8 References

1. M. I. Yehya et al., “A cost effective and light weight unipolar electroadhesion pad technology for adhesion mechanism of wall climbing robot,” *Int. j. robot. mechatron.*, vol. 2, no. 1, pp. 1–10, 2016. doi:10.21535
2. W. Saravia, “Design, Fabrication, and Testing of a Proprioceptive Electroadhesion Pad for Space Applications,” Embry-Riddle Aeronautical University, Daytona Beach, Florida, 2015.
3. G. Sebestyen, S. Fujikawa, N. Galassi, and A. Chuchra, “4.6 EPS Block Diagram,” in *Low Earth Orbit Satellite Design*, Cham, Switzerland:SPRINGER INTERNATIONAL PU, 2019, pp. 66–67.
4. T. Mooring, “FCC Online Table of Frequency Allocations,” fcc.gov, 01-Feb-2021. [Online].
5. R. Zimmerman, “OpenLST/openlst,” GitHub, 03-Aug-2018. [Online].
6. J. Chin et al., *CubeSat 101: Basic Concepts and Processes for First-Time CubeSat Developers*. NASA CubeSat Launch Initiative, 2017.
7. Shea, Garrett. “3.0 NASA Program/Project Life Cycle.” NASA, NASA, 6 Feb. 2019, <https://www.nasa.gov/seh/3-project-life-cycle>.
8. A. Thurn et al., “A Nichrome Burn Wire Release Mechanism for CubeSats,” in *Nichrome Burn Wire Release Mechanism for CubeSats.*, 2012, p. 10.
9. George I. Barsoum et al 2019 *J. Phys.: Conf. Ser.* 1264 012019 Static and Random Vibration Analyses of a University CubeSat Project